

# Designing a Computer Generated Hologram for Testing an Aspheric Surface

## 1. Introduction

Aspheric surfaces offer numerous advantages in designing optical systems. To ascertain that a fabricated asphere meets the design specifications, it has to be tested. The testing method discussed in this tutorial is known as the Computer Generated Hologram (CGH) null test. The general idea is shown in Figure 1; spherical wavefront originating from an interferometer transmits through the CGH and illuminates the aspheric mirror. If the phase of the reflected aspheric wavefront is canceled completely by the CGH then the reflected light will focus back into the interferometer. In fact the CGH acts as a certifier if the reflected light is focused back to its origin the aspheric surface passes the test; otherwise the mirror has to be polished to match the design specifications and tested again.

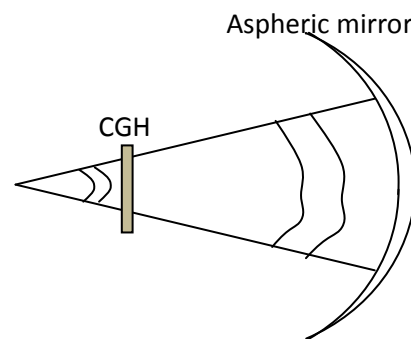


Figure 1. General CGH null test configuration

## 2. CGH Design Process

Designing the CGH involves a number of steps that are illustrated in Figure 2. The end result of this process is a CGH with wavy line pattern etched onto a chrome substrate using lithographic techniques. The process starts with optimization of the CGH in Zemax; the output of this step is a set of Zernike coefficients that define the phase function of the CGH. These coefficients would have to be converted into a 2D bit map or vector image before fabrication. This tutorial only covers the first block in the design process which is the optimization of the main CGH in Zemax.



Figure 2. CGH design steps

### 3. Design Example

In this example we use CGH to test an off axis parabolic mirror, the diagram is shown in Figure 3.

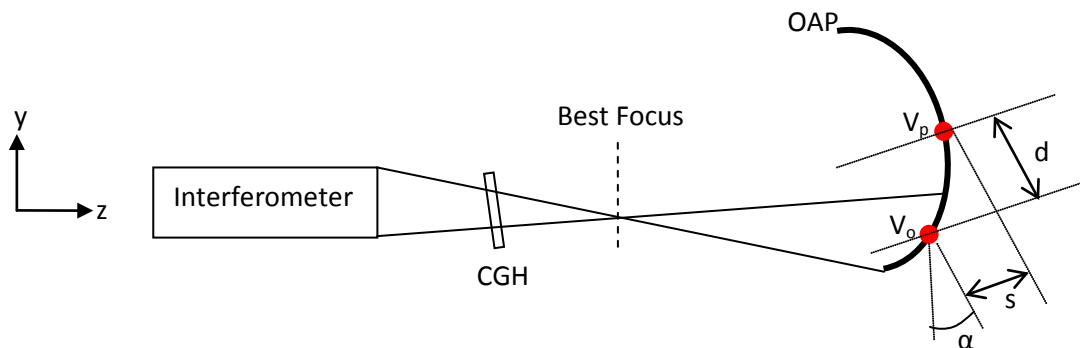


Figure 3. Diagram of the design example

Light reflected off of the CGH substrate can cause ghost fringes, therefore the CGH is tilted slightly about x axis to minimize this effect. According to this geometry light from the interferometer passes through CGH and is incident on the mirror. The mirror reflects the light back along the same path; this is known as the double pass geometry in system modeling. The residual calculation error in the simulation may result in retro reflections that do not exactly travel along the incident rays. To avoid that problem the concept of virtual glass with zero index is adopted in simulation; this concept is explained in Appendix I. The use of virtual glass allows us to model the system in three steps: single pass, phase design, and double pass. In the single pass the testing geometry is set up and the size and position of the CGH is determined. During the phase design the phase function of the CGH is calculated and optimized by setting the CGH surface type as Zernike fringe phase. In the double pass, the optical system is mirrored about the vertex of the parabolic mirror. The wavefront incident on the CGH can be compared to the wavefront emerging from it in order to validate the design.

#### 3.1. Single Pass Testing Geometry

The off axis mirror is part of a parabolic mirror with radius of curvature of 1288.1 mm, conic constant of -1 and a diameter of 562 mm. To illuminate the off axis mirror portion the coordinate system at the vertex of parabolic mirror has to be transformed to the center of the off axis mirror. The diameter of the off axis mirror  $D = 150$  mm; hence the origin of the coordinate system has to move down y axis by:

$$d = \frac{D_{parabola}}{2} - \frac{D_{off-axis}}{2} = \frac{562}{2} - \frac{150}{2} = 206 \text{ mm}$$

It needs to shift along z axis by:

$$s = \frac{d^2}{2R} = \frac{206^2}{2 * 1288.1} = 16.47 \text{ mm}$$

The coordinate system is also rotated by angle  $\alpha$  about x axis; this results in the hologram being parallel with the vertex of the off axis mirror.

$$\alpha = \arctan\left(\frac{d}{R}\right) = \arctan\left(\frac{206}{1288.1}\right) = 9.07^\circ$$

The index of refraction of the mirror is set to zero. According to the virtual glass model the refracted rays will be perpendicular to the surface of the mirror and will focus at the center of curvature. The position of the CGH determines its size. As the size of the CGH increases the spacing between the lines on the CGH pattern becomes larger which makes it more accurate but also more expensive. In this design the CGH is placed at 136 mm from best focus to minimize distortion and keep the size manufacturable. We are only concerned with the correct geometry at this point, therefore a standard surface is used for the CGH; in the next section this surface is changed to Zernike fringe phase. Operands CENX and CENY are used in merit function to insure that the x and y centroid of the ray bundle incident on the CGH surface coincide with the optical axis.

In the actual testing setup the wavefront emerging from the CGH will be spherical and converging to a point. In this setup because the CGH is placed after best focus the wavefront emerging from it will be diverging. To simulate the physical model, the CGH and best focus are mirrored along the optical axis about surface 16. The coordinate break pair on surfaces 11 and 14 tilts the CGH by about  $3^\circ$  to reduce ghost fringe effect. The surface data for the single pass geometry is listed in Table 1.

**Table 1.** Single pass surface data

Edit Solves View Help							
Surf	Type	Comment	Radius	Thickness	Glass	Semi-Diameter	Conic
OBJ	Standard		Infinity	Infinity		0.000	0.000
1	Standard	dummy surface	Infinity	100.000		75.000	0.000
STO	Standard		Infinity	0.000		75.000	0.000
3	Coordinate Br..			0.000	-	0.000	
4	Standard		Infinity	1.000	0.00,0.0	281.000	0.000
5	Standard	OAP	1288.100	0.000		281.000	-1.000
6	Standard	Comp. for Sag	Infinity	16.472		287.686	0.000
7	Coordinate Br..			0.000	-	0.000	
8	Standard		Infinity	1288.100		76.420	0.000
9	Standard	-CoC	Infinity	19.000		3.599	0.000
10	Standard	Best Focus	Infinity	136.000		2.525	0.000
11	Coordinate Br..	Reflection Control		0.000	-	0.000	
12	Standard	CGH Postion	Infinity	1.140	BK7	7.847	0.000
13	Standard		Infinity	0.000		7.890	0.000
14	Coordinate Br..	Reflection Control		0.000	-	0.000	
15	Standard		Infinity	50.000		7.890	0.000
16	Standard	Unfold illumination	Infinity	0.000	MIRROR	10.765	0.000
17	Standard		Infinity	50.000	P	10.765	0.000
18	Standard		Infinity	136.000		7.890	0.000
IMA	Standard		Infinity	-		2.443	0.000

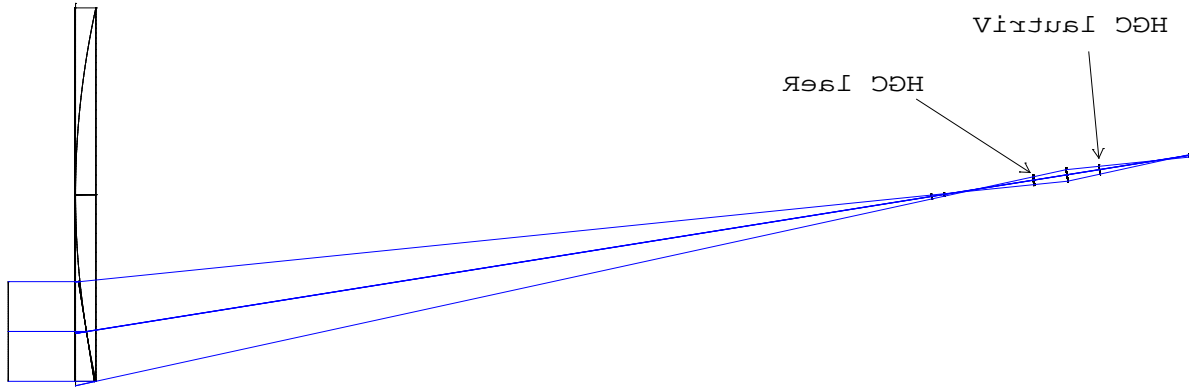


Figure 4. Layout of the single pass design

The footprint diagram at the image plane, shown in Figure 5, reveals the width of the spot size. This parameter is important since it is used to calculate the number of waves of tilt needed to separate various diffraction orders.

$$w = 0.3872 * 2 \cong 0.8 \text{ mm}$$

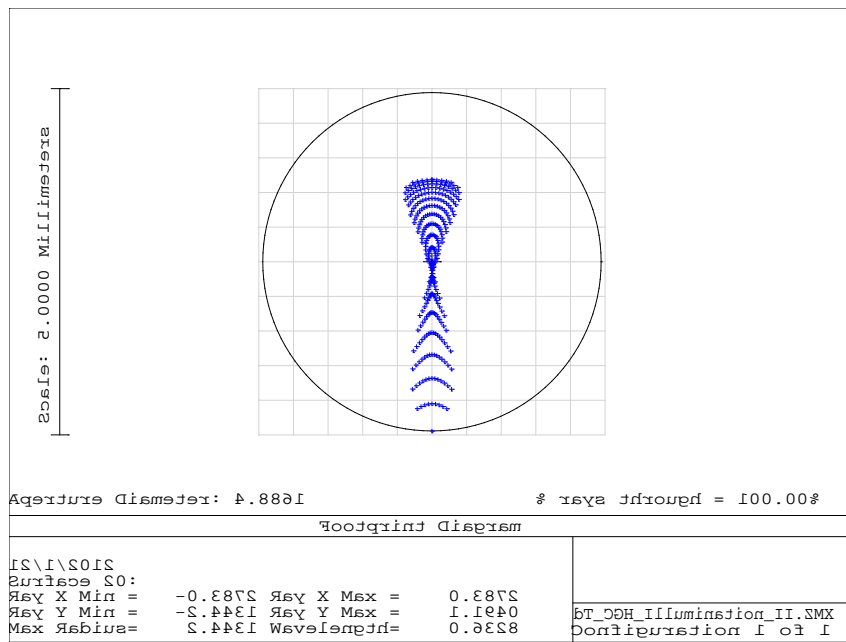


Figure 5. Footprint diagram at image plane

### 3.2. Phase Design

The phase function of CGH is modeled using the Zernike Fringe Phase surface in Zemax. The wavefront at the CGH can be expressed as a summation of the various Zernike polynomial terms with the appropriate coefficients (Appendix II). In the Extra Data Editor the maximum number of Zernike terms was specified as 36; the coefficients are normalized to the radius of the CGH surface which is 8.1mm. In order to separate the various diffraction orders some tilt must be added to the CGH. The tilt has to be carefully balanced since a large tilt drives the fabrication cost up and a small one results in overlap

among various orders. The Zernike Fringe Phase coefficient for tilt is Z2 and its value is calculated using the equation below as  $Z2 = N/2 \approx 110$ :

$$N = \frac{3}{2} w \frac{D}{\lambda * l} = \frac{3}{2} 0.8 \frac{150}{.000632 * 1307.1} = 217$$

This equation is derived in reference [4];  $N$  is the number of waves of tilt needed to separate the diffraction orders;  $w$  is the width of the spot size which was determined in the previous section as 0.8mm.  $D = 150$ mm is the diameter of test wave at the off axis parabolic mirror;  $l$  is the distance from the off axis parabolic mirror to the best focus position:

$$l = 1288.1 + 19 = 1307.1 \text{ mm}$$

The rest of the Zernike coefficients are set as variables. In the Lens Data Editor the diffraction order for the Zernike fringe phase surface is entered as +1; this results in optimization of the CGH for the +1 order. To optimize, default merit function is used which minimizes RMS spot size.

**Table 2.** Surface data for phase design

Surf>Type	Comment	Radius	Thickness	Glass	Semi-Diameter	Conic	Par 0 (unused)	
OBJ	Standard	Infinity	Infinity		0.000	0.000		
1	Standard	dummy surface	Infinity	100.000	75.000	0.000		
STO	Standard	Infinity	0.000		75.000	0.000		
3	Coordinate Br..		0.000	-	0.000			
4	Standard	Infinity	1.000	0.00,0.0	281.000	0.000		
5	Standard	OAP	1288.100	16.472	281.000	-1.000		
6	Standard	OAP Center	Infinity	0.000	284.093	0.000		
7	Coordinate Br..		0.000	-	0.000			
8	Standard	Infinity	1288.100		76.420	0.000		
9	Standard	~CoC	Infinity	19.000	3.599	0.000		
10	Standard	Best Focus	Infinity	136.000	2.525	0.000		
11	Coordinate Br..	Reflection Control		0.000	-	0.000		
12	Zernike Fring..	CGH Postion	Infinity	1.140	BK7	7.847	0.000	1.000
13	Standard		Infinity	0.000		7.897	0.000	
14	Coordinate Br..	Reflection Control		0.000	-	0.000		
15	Coordinate Br..	Order Sep. Compens.		0.000	-	0.000		
16	Standard		Infinity	50.000		7.893	0.000	
17	Standard	Unfold illumination	Infinity	0.000	MIRROR	10.795	0.000	
18	Standard		Infinity	50.000	P	10.795	0.000	
19	Standard		Infinity	136.000		7.893	0.000	
IMA	Standard		Infinity	-		0.016	0.000	

The optimized Zernike coefficients are tabulated below. These coefficients are tested in the double pass design to determine whether the actual geometry can produce a null result.

Zernike Coefficient	Value
A 1	0.00E+00
A 2	1.10E+02
A 3	0.00E+00
A 4	-3.27E+01
A 5	7.00E+01
A 6	-1.74E-01
A 7	-6.57E-02
A 8	-2.89E+01

Zernike Coefficient	Value
A 13	3.85E-04
A 14	6.89E-05
A 15	-2.50E+00
A 16	-3.94E-01
A 17	-3.07E+00
A 18	-8.31E-05
A 19	-3.30E-05
A 20	1.60E+00

Zernike Coefficient	Value
A 25	-9.49E-03
A 26	0.00E+00
A 27	-7.18E-01
A 28	-2.89E-01
A 29	-4.89E-05
A 30	-1.80E-05
A 31	7.30E-02
A 32	6.16E-03

A 9	-4.41E+00
A 10	-4.13E-04
A 11	1.24E+01
A 12	6.26E+00

A 21	6.22E-01
A 22	1.06E-04
A 23	-3.56E-06
A 24	-1.76E-01

A 33	2.35E-05
A 34	2.06E-06
A 35	-4.81E-03
A 36	5.94E-04

The default merit function minimized the RMS spot size by reducing aberrations. To insure accuracy enough sampling points must be selected in the definition of default function; in this example we used 13 rings and 12 arms. Despite the adequate amount of sampling the residual amount of aberration results in a Peak to Valley optical path difference of  $0.1\lambda$ . This number is not significant but it should not be overlooked since it indicates on the limitations of this kind of optimization. It is important to note that fitting the phase function of the CGH to Zernike polynomials is not suitable for modeling high spatial frequencies. Increasing the size of the CGH improves the Zernike fitting however if increasing the size is not an options a fitting method other than Zernike polynomial must be used.

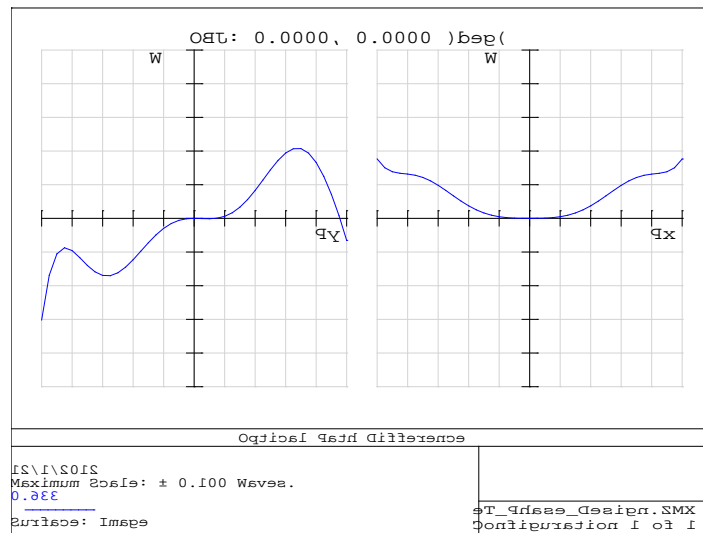


Figure 6. OPD plot at the CGH plane

### 3.3. Double Pass Testing Geometry

The double pass geometry models the physical setup. The objective here is to check the separation of various diffraction orders and determine whether they are sufficiently apart. The general approach to constructing this model is to mirror the single pass design about the y axis of the parabolic mirror. To get the correct representation, the details outlined below must be observed.

1. Start with the single pass design for which the phase function of the CGH has been optimized
2. Copy the off axis parabolic mirror (OAP) to image surface from the single pass design and paste them in reverse order
3. Follow that by pasting OAP to image surface in the same order as the single pass
4. The direction of rays in double pass is opposite of the single pass. Therefore the sign of the x axis has to flip. The signs of all rotations about the y axis need to be flipped and the sign of the diffraction order of the CGH flips from +1 to -1
5. The sign of the radius of curvature of the second OAP become negative

6. If the OAP is set as the origin of the global coordinate system the coordinates of each surface can be compared with the corresponding mirrored surface; this can be helpful in debugging the layout of the system.

**Table 3.** Surface data for double pass

Surf:Type	Comment	Radius	Thickness	Glass	Semi-Diameter	Conic		
OBJ	Standard	Infinity	0.000		0.000	0.000		
1	Standard	Infinity	136.000		0.000	0.000		
2	Standard	Infinity	50.000		8.150	0.000		
3	Standard	Unfold illumination	Infinity	MIRROR	11.147	0.000		
4	Standard		50.000		11.147	0.000		
5	Coordinate Br..	Order Sep. Compens.	0.000	-	0.000			
6	Coordinate Br..	Reflection Control	0.000	-	0.000			
7	Standard		1.140	BK7	8.154	0.000		
8	Zernike Fring..	CGH Postion	Infinity		8.100	0.000		
9	Coordinate Br..	Reflection Control	0.000	-	0.000			
10	Standard		136.000		8.105	0.000		
11	Standard	Best Focus Vorward	Infinity		5.000	U		
12	Standard	CoC	1288.100		5.270	0.000		
STO	Standard	OAP Center	Infinity		75.000	U		
14	Coordinate Br..		0.000	-	0.000			
15	Standard		16.472		282.617	0.000		
16	Standard	OAP	-1288.100	-16.472	P	MIRROR	279.618	-1.000
17	Standard	Unfold system	Infinity	0.000	MIRROR	282.644	0.000	
18	Coordinate Br..		0.000	-	0.000			
19	Standard	OAP Center	Infinity	1288.100		75.010	0.000	
20	Standard	~CoC	Infinity	19.000		3.481	0.000	
21	Standard	Best Focus Return	Infinity	136.000		5.000	U	
22	Coordinate Br..	Reflection Control	0.000	-	0.000			
23	Zernike Fring..	CGH Postion	Infinity	1.140	BK7	10.454	0.000	
24	Standard		Infinity	0.000		10.479	0.000	
25	Coordinate Br..	Reflection Control	0.000	-	0.000			
26	Coordinate Br..	Order Sep. Compens.	0.000	-	0.000			
27	Standard		Infinity	50.000		10.478	0.000	
28	Standard	Unfold illumination	Infinity	0.000	MIRROR	13.832	0.000	
29	Standard		Infinity	50.000	P	13.832	0.000	
30	Standard		Infinity	136.000		10.478	0.000	
IMA	Standard		Infinity	-		4.039	0.000	

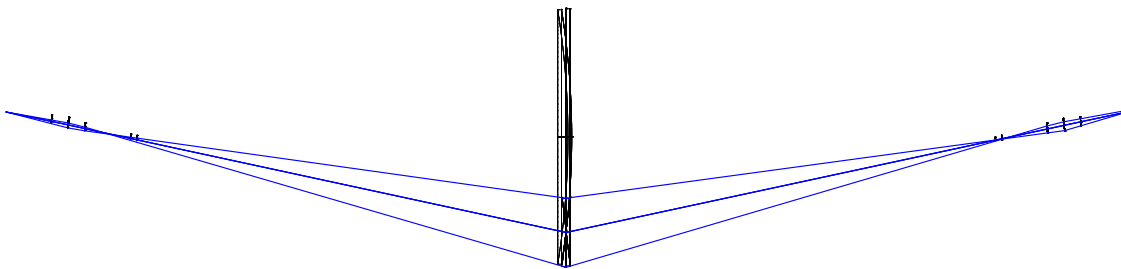


**Figure 7.** Layout of the double pass design

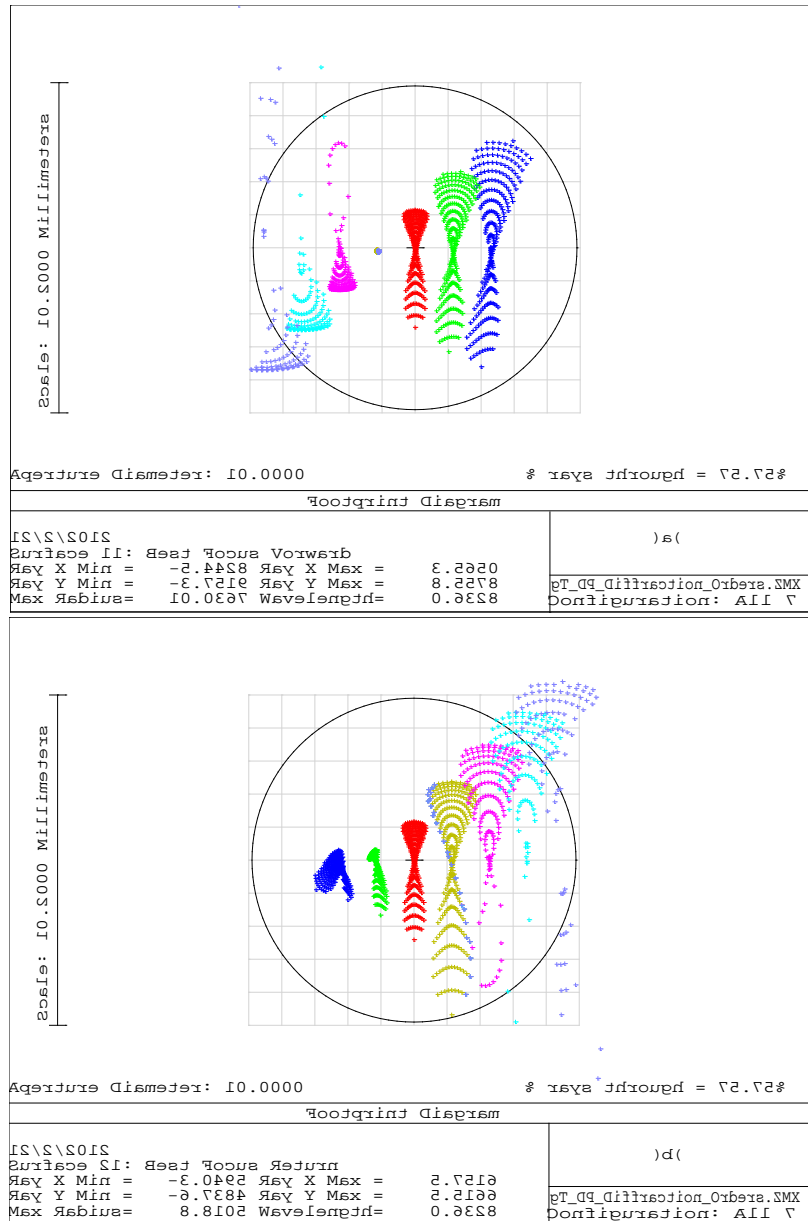


**Figure 8.** (a) Light traveling from CGH to AOP at best focus, (b) Light after reflection from AOP at best focus

Figure 8 shows the footprint diagram at the image surface for multiple diffraction orders. To generate such diagram the Multi-Configuration Editor in Zemax is set to display results for -3 to +3 diffraction orders. In diagram (a) light travels from CGH to OAP and in diagram (b) light is reflected from OAP onto the CGH and propagates through the rest of the system. The +1 diffraction order, which the phase function of the CGH was optimized for, appears in red. It separates nicely from all the other orders, has a width of 0.8 mm, and looks identical in both the forward and return diagrams. To block orders other than +1 an aperture can be placed at the best focus.



## 4. Sources of Error

The CGH design has to account for a few sources of error that arise in the fabrication and testing phase. Pattern distortion, which is the error in the positioning of the fringe lines, is an error caused by the plotter device. The wavefront error due to pattern distortion for the +1 order is:

$$\Delta W = \frac{\varepsilon}{s} \lambda$$

Where  $\varepsilon$  is pattern distortion error and  $s$  is the fringe spacing. Typical values of  $0.1 \mu\text{m}$  of pattern distortion and  $10 \mu\text{m}$  of fringe spacing result in wavefront error of  $0.01\lambda$ , which is feasible.

Misalignment of CGH during testing is another source of error. To tackle this problem, alignment marks and cross hairs are placed around the main CGH. These marks allow for accurate positioning of the CGH with respect to the interferometer beam and the rest of the setup. The alignment hologram is designed simultaneously with the main hologram and it is an essential component of the CGH for practical testing purposes. The procedure for designing the alignment CGH was not covered in this tutorial, for more information on this topic review reference [6].

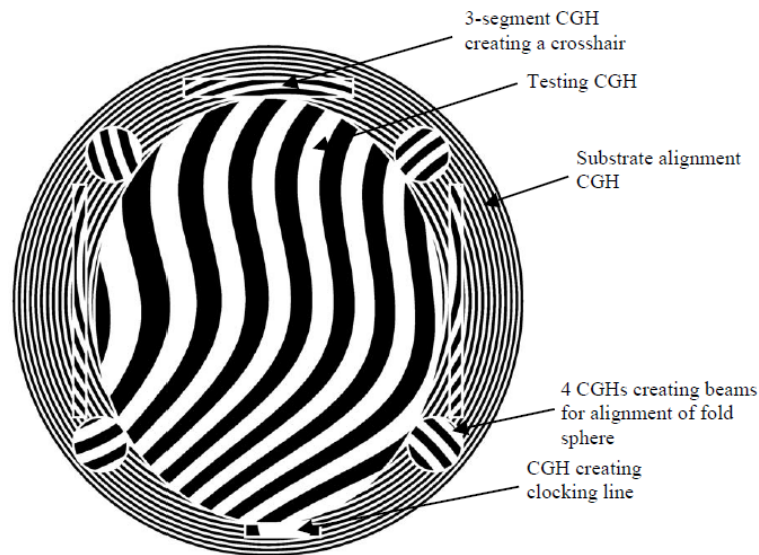


Figure 9. Testing and Alignment CGH on a single substrate [6]

## 5. Conclusion

In this tutorial the phase function of CGH was optimized for a particular geometry in which an off axis parabolic mirror was being tested. The process was carried out in three steps; a few lens design tricks such the virtual glass concept and the mirroring of best focus were employed to ease the difficulties in modeling a physical setup. The CGH was optimized for the +1 order which separates well from the other diffraction orders and maintains its profile. An important practical consideration that was not discussed was the diffraction efficiency which for a typical amplitude hologram is about 10%. The output of this tutorial is an optimized phase function for the CGH. The next step in realizing the CGH is to convert the phase function to a 2D line pattern that can be plotted and etched on a chrome substrate. However prior to converting the phase function, alignment CGH must be added to the testing CGH to assist with the accurate placement of the fabricated CGH in the testing setup.

## Appendix I – Virtual Glass

Figure 10 shows the schematic for a virtual glass; light from infinity is incident on the glass with zero index. To satisfy Snell's law

$$n_1 \sin \theta_1 = n_2 \sin \theta_2$$

for  $n_1 = 0$ ,  $\sin \theta_2$  has to equal zero which means  $\theta_2 = 0$ , hence the refracted ray is perpendicular to the aspheric surface. This trick allows us to analyze the system in single pass, optimize the design, determine the parameters and apply those to the double pass system for a complete treatment of the problem.

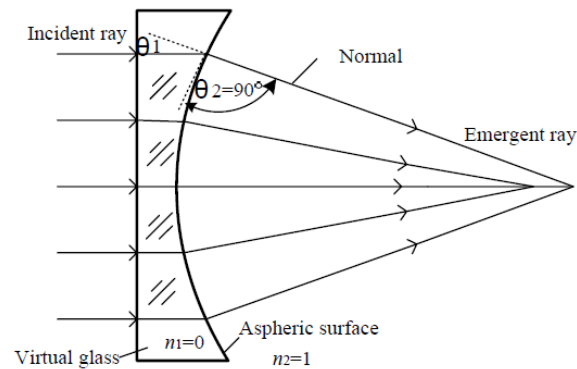


Figure 10. Schematic of a virtual glass

## Appendix II – Zernike Fringe Phase Surface

The generalized form of the wavefront function expanded in terms of the Zernike polynomial is:

$$\Phi = M \sum_{i=1}^N 2\pi A_i Z_i(\rho, \varphi)$$

M is the diffraction order of the CGH which is specified as +1 in this simulation. N is the number of Zernike terms, which Zemax supports up to 37, all of which are used in this optimization.  $Z_i(\rho, \varphi)$  is the  $i^{\text{th}}$  term in the Zernike polynomial series and  $A_i$  is the coefficient of that term in units of waves.  $Z_i$  is the function of  $\rho$  which is the normalized radial ray coordinate and  $\varphi$  which is the angular ray coordinate

$A_i$	$Z_i(\rho, \varphi)$
$A_1$	1
$A_2$	$\rho \cos(\varphi)$
$A_3$	$\rho \sin(\varphi)$
$A_4$	$2\rho^2 - 1$
$A_5$	$\rho^2 \cos(2\varphi)$
$A_6$	$\rho^2 \sin(2\varphi)$
$A_7$	$(3\rho^2 - 2)\rho \cos(\varphi)$
$A_8$	$(3\rho^2 - 2)\rho \sin(\varphi)$
$A_9$	$(6\rho^4 - 6\rho^2 + 1)$
$A_{10}$	$\rho^3 \cos(3\varphi)$
$A_{11}$	$\rho^3 \sin(3\varphi)$
$A_{12}$	$(4\rho^2 - 3)\rho^2 \cos(2\varphi)$
$A_{13}$	$(4\rho^2 - 3)\rho^2 \sin(2\varphi)$
$A_{14}$	$(10\rho^4 - 12\rho^2 + 3)\rho \cos(\varphi)$
$A_{15}$	$(10\rho^4 - 12\rho^2 + 3)\rho \sin(\varphi)$
$A_{16}$	$(20\rho^6 - 30\rho^4 + 12\rho^2 - 1)$
$A_{17}$	$\rho^4 \cos(4\varphi)$
$A_{18}$	$\rho^4 \sin(4\varphi)$

$A_i$	$Z_i(\rho, \varphi)$
$A_{19}$	$(5\rho^2 - 4)\rho^3 \cos(3\varphi)$
$A_{20}$	$(5\rho^2 - 4)\rho^3 \sin(3\varphi)$
$A_{21}$	$(15\rho^4 - 20\rho^2 + 6)\rho^2 \cos(2\varphi)$
$A_{22}$	$(15\rho^4 - 20\rho^2 + 6)\rho^2 \sin(2\varphi)$
$A_{23}$	$(35\rho^6 - 60\rho^4 + 30\rho^2 - 4)\rho \cos(\varphi)$
$A_{24}$	$(35\rho^6 - 60\rho^4 + 30\rho^2 - 4)\rho \sin(\varphi)$
$A_{25}$	$(70\rho^8 - 140\rho^6 + 90\rho^4 - 20\rho^2 + 1)$
$A_{26}$	$\rho^5 \cos(5\varphi)$
$A_{27}$	$\rho^5 \sin(5\varphi)$
$A_{28}$	$(6\rho^2 - 5)\rho^4 \cos(4\varphi)$
$A_{29}$	$(6\rho^2 - 5)\rho^4 \sin(4\varphi)$
$A_{30}$	$(21\rho^4 - 30\rho^2 + 10)\rho^3 \cos(3\varphi)$
$A_{31}$	$(21\rho^4 - 30\rho^2 + 10)\rho^3 \sin(3\varphi)$
$A_{32}$	$(56\rho^6 - 105\rho^4 + 60\rho^2 - 10)\rho^2 \cos(2\varphi)$
$A_{33}$	$(56\rho^6 - 105\rho^4 + 60\rho^2 - 10)\rho^2 \sin(2\varphi)$
$A_{34}$	$(126\rho^8 - 280\rho^6 + 210\rho^4 - 60\rho^2 + 5)\rho \cos(\varphi)$
$A_{35}$	$(126\rho^8 - 280\rho^6 + 210\rho^4 - 60\rho^2 + 5)\rho \sin(\varphi)$
$A_{36}$	$(252\rho^{10} - 630\rho^8 + 560\rho^6 - 210\rho^4 + 30\rho^2 - 1)$
$A_{37}$	$(924\rho^{12} - 2772\rho^{10} + 3150\rho^8 - 1680\rho^6 + 420\rho^4 - 42\rho^2 + 1)$

## References

1. Jie Feng, Chao Deng, Tingwen Xing, "Design of Aspheric Surfaces Testing System Based on Computer-generated Holograms", Proc. of SPIE Vol. 8418 (2012)
2. Jiang Yi, Wang Ping, Qi Yuejing, Wei Nan, "Compensator Design for Aspheric Testing using Virtual Glass Model", Proc. of SPIE Vol. 6723 (2008)
3. Dae Wook Kim, "Computer Generated Holography Workshop", University of Arizona College of Optical Sciences (2012)
4. Dr. Jim Burge, "Computer Generated Holograms for Optical Testing", University of Arizona College of Optical Sciences
5. James H. Burge and James C. Wyant, "Use of Computer Generated Holograms for Testing Aspheric Optics", University of Arizona College of Optical Sciences
6. Rene Zehnder, James H. Burge and Chunyu Zhao, "Use of computer generated holograms for alignment of complex null correctors", University of Arizona College of Optical Sciences